Riboflavin-Vancomycin Conjugate Enables Simultaneous Antibiotic Photo-Release and Photodynamic Killing against Resistant Gram-Positive Pathogens

Bethany Mills,[#*2] Alex Kiang, [#2] Syam Mohan P. C. Mohanan,[2] Mark Bradley,[1] and Maxime Klausen*[1]

1 Prof. M. Bradley, Dr. M. Klausen
EaStCHEM School of Chemistry, University of Edinburgh, David Brewster Road, EH9 3FJ Edinburgh, UK.
E-mail: mklausen@ed.ac.uk

2 Dr. B. Mills, A. Kiang, Dr. S. M. P. C. Mohanan
Translational Healthcare Technologies group, Centre for Inflammation Research, Queen's Medical Research Institute, University of Edinburgh, 47 Little France Crescent, Edinburgh EH16 4TJ, UK.
E-mail: beth.mills@ed.ac.uk

[#] Authors contributed equally

Supporting information for this article is given via a link at the end of the document.

Abstract: Decades of antibiotic misuse have led to alarming levels of antimicrobial resistance, and the development of alternative diagnostic and therapeutic strategies to delineate and treat infections is a global priority. In particular, the nosocomial, multi-drug resistant "ESKAPE" pathogens such as Gram-positive methicillin resistant *Staphylococcus aureus* (MRSA) and vancomycin resistant *Enterococcus spp* (VRE) urgently require alternative treatments. Here, we developed light-activated molecules, based on conjugation of the FDA-approved photosensitizer riboflavin to the Gram-positive specific ligand vancomycin, to enable targeted antimicrobial photodynamic therapy. The riboflavin-vancomycin conjugate proved to be a potent and versatile antibacterial agent, enabling the rapid, light-mediated, killing of MRSA and VRE with no significant off-target effects. The attachment of riboflavin on vancomycin also led to an increased in antibiotic activity against *S. aureus* and VRE. Simultaneously, we evidenced for the first time that the flavin sub-unit undergoes an efficient photo-induced bond cleavage reaction to release vancomycin, thereby acting as a photo-removable protecting group for drug-delivery.

Introduction

The emergence of antimicrobial resistant (AMR) and multi-drug resistant (MDR) bacteria has been exacerbated by the misuse and overuse of antibiotics, and pose a major threat to human health.[1,2] In particular, the emergence of the nosocomial, MDR "ESKAPE" pathogens (*Enterococcus spp.; Staphylococcus aureus; Klebsiella pneumoniae; Acinetobacter baumanii; Pseudomonas aeruginosa* and *Enterobacter spp.*), [3] which have been designated as "critical" and "high priority" for the development of alternative treatments by the World Health Organisation (WHO)[4] are a significant cause for concern. Importantly, a dozen novel antibiotics have been approved in the past five years,[5] however, resistance development remains a fast-paced issue global issue,[6,7] and there is a constant and urgent need to develop approaches that move beyond the classical bactericidal pathways.[8] Photodynamic therapy (PDT) offers great potential in this regard.[8-10] PDT relies on the administration of a photosensitizer (PS), which generates a range of reactive oxygen species (ROS) upon absorption of specific wavelengths of light.[11-13] Following absorption, the PS molecule undergoes intersystem-crossing from a singlet excited state to a long-lived triplet state, which enables the generation of ROS in the form of hydroxyl radicals (Type I photo-process) and/or singlet oxygen (Type II photo-process). The high and localised toxicity of these short-lived species has been widely exploited for the treatment of cancer,[14] skin[15,16] and oral diseases.[17,18] However, applications for PDT have the potential to extend far beyond these, and are particularly attractive in the context of infection; especially when aimed towards topical infections amenable to light delivery such as those of the skin (wounds, burns, and diabetic foot ulcers), cornea, surgical sites, or the oral cavity, for which Gram-positive bacteria including methicillin resistant *S. aureus* (MRSA) and vancomycin resistant *Enterococcus spp.* (VRE) remain clinical challenges.

Antimicrobial PDT (aPDT) has the potential to become a sustainable alternative to standard antibiotic treatment as pathogens are considered unlikely to develop resistance mechanisms to the lethal and fast-acting ROS generated by the PS.[19] The challenge however lies in the design of photosensitizing drugs with a high therapeutic index to limit off-target photo-toxicity against healthy mammalian cells.[10,20] Cationic PS which bind non-specifically to negatively charged microbial membranes have been successfully deployed in aPDT[21-23] However, clinical aPDT remains at an early stage of development compared to anticancer PDT,[24,25] partly because of poor pathogen selectivity.

Among the strategies to augment photosensitizing drug specificity, is the covalent conjugation of PS molecules to pathogen-specific ligands to enable direct binding to microbes. We have previously demonstrated targeted aPDT eradication of Gram-negative bacteria with a probe based on a Methylene Blue PS conjugated to a modified polymyxin B scaffold[26] allowing generation of ROS in direct proximity of the pathogens. Here we aimed to expand the aPDT toolbox by designing and synthesizing a novel, complementary aPDT probe to target Gram-positive bacteria, and

validate it against pathogens including MRSA and VRE. Our Gram-positive-specific aPDT agent was designed as a covalent conjugate of the glycopeptide antibiotic vancomycin as the binding ligand, and riboflavin (vitamin B2) as the PS. Riboflavin was selected due to its high bio-compatibility, low cost and FDA-approved status while its singlet oxygen quantum yield (Φ_Δ) of 0.54,[27] shows high ROS generation efficiency. The riboflavin-vancomycin conjugate led to complete photodynamic-mediated killing of MDR Gram-positive infections after only 20 minutes of illumination. During our investigation, we also discovered for the first time that the flavin chromophore acts as a photo-removable protecting group (PPG)[28,29] for amine groups via photo-cleavage of its side chain, which here led to concomitant vancomycin release during the course of the aPDT treatment. Although the photo-sensitivity of vitamin B2 via radical side-chain oxidation has been known for decades,[30,31] this is the first example of a modified riboflavin showing properties as a PPG for amines, which makes it a useful scaffold for applications in both PDT and light-mediated drug-delivery.

Results and Discussion

Chemical Synthesis and Characterisation

In order to achieve high Gram-positive bacteria selectivity, the targeted photosensitizing agent was designed by modifying vancomycin on its amino-glycan moiety by reductive amination; a strategic modification used to tune the potency of glycopeptides for resistant Gram-positive bacteria, as demonstrated in derivatives such as oritavancin.[32] The preparation of the PDT probe was carried out in an efficient two-step synthesis starting from vitamin B2 (Scheme 1). The poly-ol side-chain of riboflavin was cleaved under oxidative conditions to yield aldehyde 1, which was directly attached to vancomycin hydrochloride by reductive amination.[33] This sequence afforded the target aPDT probe **VanB2** on gram scale and the new light-activated probe was fully characterized by NMR, HPLC, HRMS and MALDI-TOF MS (see SI).

The absorption and emission properties of the aPDT probe **VanB2** (Table 1) were in accordance with unconjugated riboflavin, with a large absorption band at 444 nm and an absorption coefficient of 1.2 10^4 $M^{-1}cm^{-1}$ at this wavelength in PBS, and similar properties in MeOH and DMSO. The **VanB2** conjugate retained a residual green emissive character (Φ_f = 0.02), albeit much less bright than unmodified riboflavin (Φ_f = 0.27).[34] The generation of ROS was investigated via irradiation of the probe (10 μM) at 470 nm (4.0 mW/cm^2) in presence of ROS chemical traps, and comparing the results with unmodified riboflavin under the same experimental conditions. Irradiation in presence of the water-soluble $^1O_2$ sensor 9,10-Anthracenediyl-bis(methylene)dimalonic acid (ABMDMA, 100 μM) showed a decrease in absorbance at 380 nm (Fig. 1, Fig. S2-S3), indicating the formation of the corresponding endo-peroxide generated after the formation of singlet oxygen (Scheme S1).

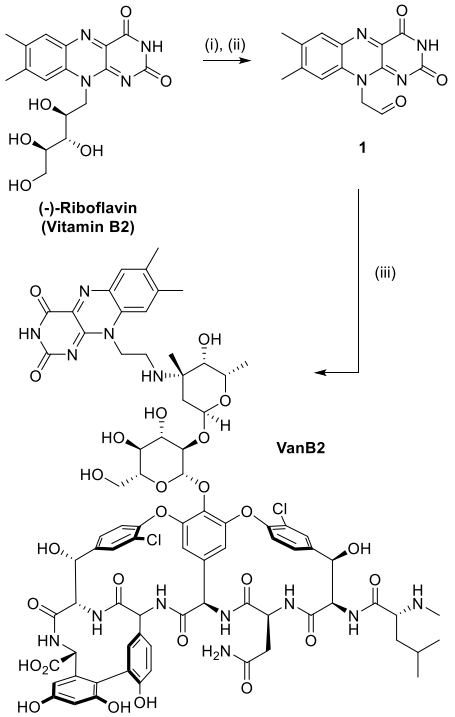

Scheme 1. Synthesis of VanB2. Reagents and conditions: (i) $NaIO_4$, H_2O, r.t., 16 h. (ii) Toluene, reflux, 4 h. (iii) Vancomycin hydrochloride, DIPEA, DMF, $NaBH_3CN$, MeOH, TFA, r.t., 16 h.

The kinetics and quantification of the $^1O_2$ trapping were monitored (Fig. 1, c), which allowed determination of the relative rates of $^1O_2$ generation, and the corresponding $^1O_2$ quantum yields Φ_Δ (see SI). The absorbance band of ABMDMA disappeared after only 40 s in presence of the reference riboflavin, but only by 12 % in presence of **VanB2**, leading to a comparative Φ_Δ of 0.16. Type-I photo-processes were also investigated using dihydrorhodamine 123 (DHR 123, 10 μM in water), and monitoring the increase in fluorescence at 526 nm upon oxidation of DHR123 to rhodamine 123 (Scheme S2), which led to a similar pattern (Fig. 1, d, and Fig. S4-S5). This is a first indication that the modification of the riboflavin side-chain strongly affect the relaxation processes from the excited state. Since the π-conjugated system of the PS was not modified during the synthesis, intramolecular interactions such as excited-state hydrogen bonding are likely to be the cause of the drop of Φ_Δ. The $^1O_2$ generation promoted by the probe also proved to be highly sensitive to the environment, with 4-fold higher Φ_Δ values in MeOH compared to PBS (Table 1, Fig. S1). Interestingly, in DMSO, which is known to react with singlet oxygen to form dimethylsulphone,[35] the irradiation experiments evidenced clearly the photo-degradation of the riboflavin unit without oxidation of the ABMDMA sensor (Fig. S1). This degradation under blue-light was then further investigated.

Table 1. Photophysical properties of VanB2 in different solvents.

Solvent	λ_{abs}^{max} (nm)	ε^{max} (M^{-1} cm^{-1})	λ_{em}^{max} (nm)	Stokes shift (cm^{-1})	ϕ_f[a]	ϕ_Δ[b]
MeOH	439	1.0×10^4	512	3247	0.23	0.71
DMSO	442	1.3×10^4	510	3017	0.08	--[c]
PBS	444	1.2×10^4	528	3583	0.02	0.16

[a] Fluorescence quantum yield measured upon excitation at the maximum of the riboflavin absorption band, relative to Fluorescein in NaOH 0.1 M (Φ_f = 0.90). [b] Singlet oxygen quantum yield, determined by a relative measurement method; upon irradiation at 470 nm (4.0 mW/cm^2) in the presence of the singlet oxygen sensor ABMDMA (100 μM) and comparison with (-)-Riboflavin under identical conditions (see SI for details). [c] Only degradation of the riboflavin ring was observed.

Vancomycin release via riboflavin photo-cleavage

The irradiation experiments performed with **VanB2** evidenced a "self-destructive" character under blue light, with the absorbance value of **VanB2** in PBS decreasing by 50 % after 3 minutes of irradiation (Fig. 2, b). In order to understand the structural modifications at play in this apparent bleaching mechanism, the photolysis of **VanB2** was performed in PBS, monitoring the reaction by UV-Vis spectroscopy and HPLC-MS. During the course of the irradiation, HPLC showed the disappearance of the peak corresponding to **VanB2**, and the appearance of two photo-products at 2.16 and 3.37 min (Fig. 2, c) that were attributed respectively to vancomycin and lumichrome, a known by-product of riboflavin photolysis, via the intermediate aldehyde **1**.[30,31] Products were identified both by LC-MS (Fig. S6), and individual injection of the corresponding standards. This confirms that the linker between vancomycin and riboflavin is cleaved in a photochemical cascade, thereby releasing the vancomycin scaffold (Fig. 2, a). The concomitant formation of lumichrome, a blue-shifted flavin derivative (λ_{abs}^{max} = 385 nm), as by-product of the cleavage is also in accordance with the UV-Vis monitoring of the photolysis (Fig. 2, b) showing a decrease in the absorbance of **VanB2** at 440 nm and an increase in the intensity of the 380 nm band. Control experiments confirmed that solutions of lumichrome do not generate singlet oxygen with blue light (Fig. S7),

Monitoring the release of the caged vancomycin upon irradiation by HPLC allowed determination of several key parameters of the photolytic reaction. HPLC quantification (Fig. S8) showed that the chemical yield of the photo-release of vancomycin was >90%, with the photocleavage reaction following first order kinetics in PBS (Fig. S9). The rate of the reaction was essentially unaffected when the photolysis was performed under anaerobic conditions (i.e. under continuous nitrogen flow, see SI), proving the reaction to be oxygen-independent, and therefore not singlet-oxygen mediated.

Kinetic analysis allowed determination of the photochemical quantum yield of this new uncaging reaction. The uncaging quantum yield (Φ_u) is defined as the number of "caged" molecules released per 100 photons absorbed - which is indicative of the photochemical efficiency of the bond cleavage.

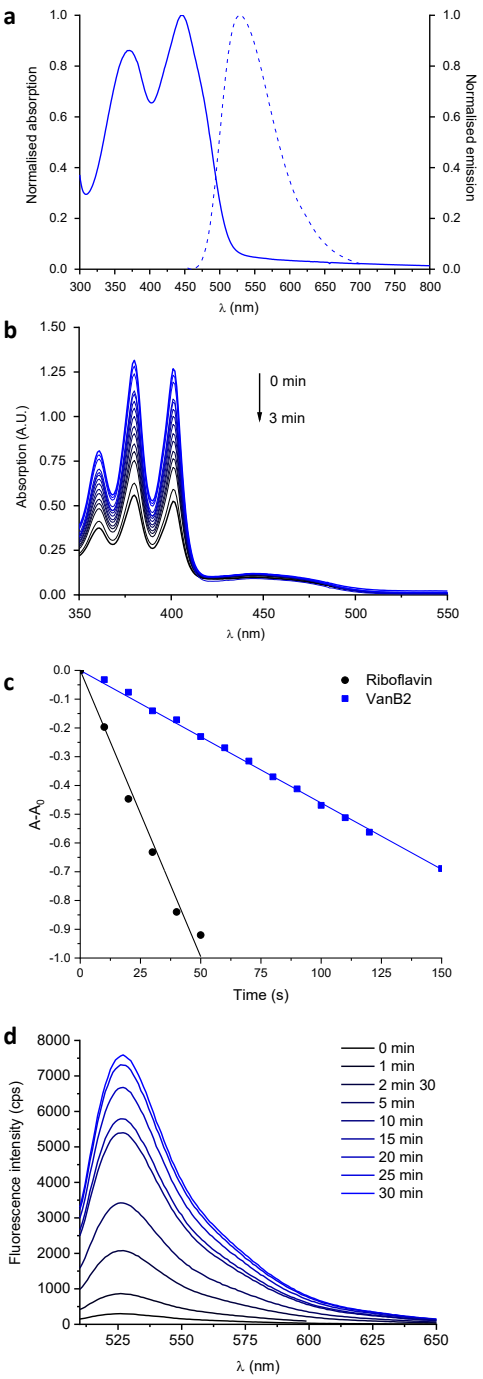

Figure 1. Optical properties and singlet oxygen generation of the new PS agents in PBS. (a) Normalised absorption (continuous) and emission (dashed) spectra of VanB2. Fluorescence spectra were recorded at the maximum of excitation of the riboflavin band according to the values reported in Table 1. (b) Evolution of the absorption spectrum of a PBS solution containing the $^1O_2$ sensor ABMDMA and VanB2 upon excitation at 470 nm over 3 min. (c) Kinetics of the decrease in absorbance of the ABMDMA sensor at 380 nm over time during irradiation in the presence of riboflavin (reference, black circles) and VanB2 (blue squares). (d) Evolution of the fluorescence spectrum of a PBS solution containing the ROS sensor DHR123 and VanB2 upon excitation at 470 nm over 30 min.

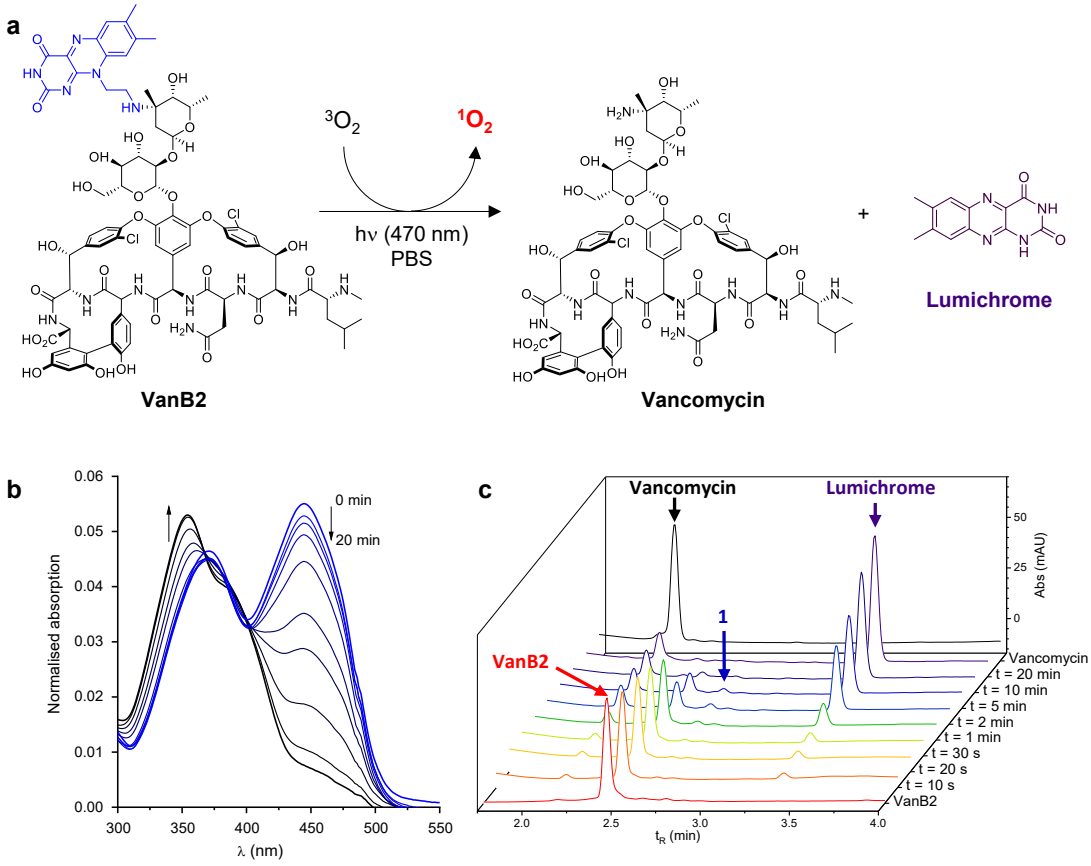

Figure 2. (a) Photolysis reaction occurring during the irradiation of VanB2, with the independent generation of singlet oxygen and the cleavage of the riboflavin "protecting group". (b) Evolution of the absorbance spectrum during 20 min of irradiation (470 nm) of VanB2 in PBS, showing the disappearance of the riboflavin band at 440 nm and the appearance of an absorbance at 350 nm due to lumichrome. (c) HPLC time course (detection at 254 nm) of the photolysis products of VanB2 (2.5 μM, 470 nm) showing the formation of vancomycin and lumichrome with intermediate formation of aldehyde 1.

The Φ_u value is known to be directly related to the kinetics of the uncaging reaction (see SI) and to the total irradiation intensity I at 470 nm, which was measured using the potassium ferrioxalate chemical actinometry method (see SI).[36] Using the rate constant determined from kinetic analysis, the photochemical quantum yield Φ_u of vancomycin uncaging could be determined. A value of $\Phi_u = 0.0027$ was obtained, which was in good agreement with the photochemical-dissociation quantum yield reported for the cleavage of the side chain of natural riboflavin in phosphate buffer ($\Phi_{diss} = 0.0078$ [37]).

The photo-cleavable character evidenced in **VanB2** is likely the result of a triplet diradical formed in the excited state. In natural vitamin B2, this diradical evolves towards the oxidative cleavage of the poly-ol side-chain and the formation of aldehyde **1**.[30,31] The formylmethyl moiety can then be further cleaved at neutral and acidic pH to yield lumichrome and glycolaldehyde.[31] Although further mechanistic investigation is required, the transient formation of aldehyde **1** evidenced by HPLC-MS indicates that **VanB2** likely follows a similar diradical pathway, where the ethylamine linker hereby releases the caged amine instead of the hydroxyl side-chain in natural riboflavin. In the present case, the diradical cascade may initially involve the formation of an imine which would then be hydrolysed to aldehyde **1** and vancomycin. Lumichrome and glycolaldehyde would then be formed according to the reported degradation mechanism.[31] Additional photolysis experiments were performed in deuterated solvents, following the evolution of the ^{1}H NMR spectra of **VanB2** over the course of the irradiation. Interestingly, the photocleavage did not proceed in pure D_2O, only starting upon the addition of a trace of acid. This indicates that the release mechanism in aqueous media is likely pH dependant, which supports the hypothesis of it proceeding via possible imine hydrolysis. Photolysis in DMSO-d_6 (Fig. S10) confirmed the formation of free vancomycin (representative singlet at 7.86 ppm, in addition to the rest of the signals matching the reported assignment in DMSO-d_6 [38]) and the simultaneous release of lumichrome (singlets appearing at 7.90 and 7.71 ppm) during the course of the irradiation. No further reaction intermediates or by-products were identified.

This finding shows that the flavinylethyl scaffold behaves as a new light cleavable protecting group, and is able to uncage a bio-active molecule via a protected amine group under blue light irradiation. This indicates that a stoichiometric dose of vancomycin will be released in parallel to the PDT treatment, which opens avenues into combinatorial therapy strategies where the release of various

payloads can be envisioned. Solutions of **VanB2** in PBS also proved to be very robust in the dark. No modification of the absorption spectra or HPLC traces were observed after 1 year of storage at -20 °C, and solutions of the compound stored at room temperature were still 82% pure after a month (Fig. S11). This indicates no competitive dark cleavage or degradation occurs in water and is crucial for potential translation to clinical applications.

VanB2 killing of Gram-positive bacteria

The sensitivity, specificity and phototoxic antibacterial properties of **VanB2** against target (Gram-positive bacterial strains *S. aureus* and vancomycin resistant *E. faecalis*), and off-target (Gram-negative *E. coli*) bacteria were determined, and compared to equimolar concentrations of natural riboflavin and vancomycin. The compounds (5 μM) were incubated with the bacteria for 10 min (washing away excess compound), followed by either 20 min illumination (455 nm LED, 30 mW/cm^2, Fig. S12) or maintained in the dark to prevent photoactivation of the probe. Following PDT treatment with **VanB2**, no Gram-positive bacterial colonies were recovered when plated for colony forming units (CFUs), marking a 7-log reduction (P < 0.0001) in CFU mL^{-1} compared to **VanB2** labelled bacteria maintained in the dark, riboflavin controls (with and without illumination) and PS-free controls (Fig. 3). *E. coli* remained unaffected by any treatment, even with **VanB2** in excess (Fig. 3, d). This suggests that any ROS generated within the surrounding microenvironment was too diffuse to yield an off-target biological response, demonstrating the importance of locking onto the target pathogen.

A dose response of **VanB2** phototoxicity against *S. aureus* determined that 0.63 μM caused complete killing following illumination, whilst the effect was lost at 0.16 μM, with an intermediate level of killing observed at 0.31 μM (Fig. S13). There was no killing induced by riboflavin, or the vancomycin controls, in the dark or following illumination, even at 10 μM, on the short exposure involved for the aPDT experiments (i.e. 30 min). On this short timescale, *S. aureus* remained unaffected by the contact with vancomycin despite being sensitive to the antibiotic at concentrations less than 3 μM (<5 μg mL^{-1}, determined by conventional minimum inhibitory concentration (MIC) assay (Table S1)).

When applied in non-photodynamic situations (i.e. conventional antibiotic action over 15 h), the antibiotic activity of **VanB2** (Fig. S14) was also enhanced over vancomycin. Whilst only 10 μM vancomycin caused complete growth inhibition of *S. aureus*, both 10 μM and 1 μM **VanB2** totally inhibited growth rate of *S. aureus* through its antibiotic activity (in the dark). This enhanced activity can be explained by the introduction of the aromatic riboflavin subunit on the vancosamine position which is known to enhance potency, and is consistent with the reduced MIC observed in other arylated vancomycin derivatives (e.g. oritavancin).

We further sought to characterise the aPDT and antibiotic potency of **VanB2** against bacteria strains expressing vancomycin resistance. The vancomycin resistant *E. faecalis* strain utilised here possessed Van-B mediated resistance, which confers a modified peptidoglycan structure (where D-Ala-D-Ala is replaced by D-Ala-D-Lac in peptidoglycan cell-wall precursors)[39] and reduces the binding affinity of vancomycin.[40] The vancomycin resistance was confirmed with an MIC value between 34 – 68 μM (Table S1).

Figure 3. Colony forming units (CFU) of bacteria following aPDT treatment with VanB2 or riboflavin. Gram-positive bacteria (a) *S. aureus*; (b) Vancomycin resistant *E. faecalis*; and (c) Gram-negative bacteria *E. coli* were incubated with VanB2 or riboflavin (5 μM) for 10 min prior to removal of excess compound followed by 20 min illumination (4550 nm, 30 mW/cm^2). Controls were maintained in the dark with or without compound. All samples were plated for colony forming units (CFU) to determine bacterial survival. (d) *E. coli* was treated as in (c) without removal of excess compound prior to illumination. (e) CFU and photograph of *S. aureus* strains with differential expression of staphyloxanthin (orange-yellow pigment) following aPDT with VanB2 (and dark controls). Error bars show s.e.m., (a-d) analysed one-way ANOVA with comparison to (a-d) bacteria-only control or (e) dark control: ****P < 0.0001. n = 3.

Despite this, **VanB2** proved to be proficient aPDT agent against the VRE strain. Complete *E. faecalis* killing was achieved using 1.25 μM of the probe, within 20 min of illumination, rendering a 7-log reduction in cell viability ($P < 0.0001$) (Fig 3b, Fig. S13). This was twice the concentration required for the same CFU reduction of *S. aureus* under the same experimental conditions, which suggests a modest reduction in **VanB2** susceptibility, possibly due to a reduced binding affinity consistent with the mechanism of vancomycin resistance.

Additionally, the non-light based, antibiotic potency of **VanB2** against vancomycin-resistant strains proved to be significant, completely preventing growth of VRE over 15 h at 10 μM, and partially slowing it at 1 μM (Fig. S14). This indicates that the vancosamine modification with riboflavin is a powerful strategy not only to strongly increase the potency of vancomycin derivatives, but also to bypass Van-B resistance mechanisms.

Finally, bacteria also have a number of virulence factors that may protect them from exogenous ROS.[41] In particular, *S. aureus* has a variety of defence mechanisms which are upregulated following oxidative burst, such as antioxidant enzymes and small molecules.[42] We evaluated **VanB2** against a panel of *S. aureus* strains (including methicillin resistant strain MRSA USA300), which exhibited a range of staphyloxanthin pigmentation. Staphyloxanthin is a membrane-bound anti-oxidant carotenoid responsible for the yellow-orange appearance of many *S. aureus* strains. It is believed to offer protection against oxidative stress, including by impairing neutrophil ROS mediated killing through its ability to scavenge hydroxyl radicals, with strains lacking the pigment more easily killed.[43] Here, aPDT mediated killing with **VanB2** was shown to be independent of staphyloxanthin carotenoid levels (Fig. 3, e). These results show that **VanB2** remains an efficient photo-therapeutic agent against AMR pathogens, including in presence of high concentrations of ROS-scavenging species.

Together, the selective, rapid and efficient nature of **VanB2** mediated aPDT against drug resistant Gram-positive bacteria was demonstrated even at low concentrations, which was not achievable by PS or antibiotic alone. The combined aPDT and secondary conventional antimicrobial activity of **VanB2** could provide an important alternative treatment for wound infections caused by *E. faecalis*.[44]

Subcellular imaging of VanB2 treated Gram-positive bacteria

Transmission electron microscopy (TEM) of *S. aureus* and *E. faecalis* following treatment with **VanB2** under blue light irradiation (along with untreated controls) was performed, with bacteria fixed immediately after PDT treatment. A number of morphological changes were observed across the **VanB2** treated bacteria compared to controls (Fig. 4). Post-treatment, *S. aureus* were shown to have a number of disruptions to the cell envelope and overall shape, including irregular cell envelope thickness, breaks in the plasma membrane and rougher cell-surfaces. Unlike the untreated bacteria, very few of the treated *S. aureus* cells had visible septum, and those which were visible were distorted. Furthermore, internal "mesosome-like" structures were observed only in PDT treated cells. The association between mesosome-like structures and ROS[45] or antibiotic (including vancomycin) damage within bacteria has been previously reported, and these were a consistent feature of our **VanB2** and LED treated *S. aureus*. TEM images of the **VanB2** treated *E. faecalis* showed similar cell envelope damage, and demonstrated major intracellular changes after treatment, with the formation of electron-dense aberrant structures and septum deformities. Occasional "ghost" cell envelope structures were also observed, indicating separation of the cell wall from the protoplast. Photo-activated **VanB2** is therefore able to elicit extracellular and intracellular cell damage through $^1O_2$ diffusion across bacterial cell wall and plasma membranes.

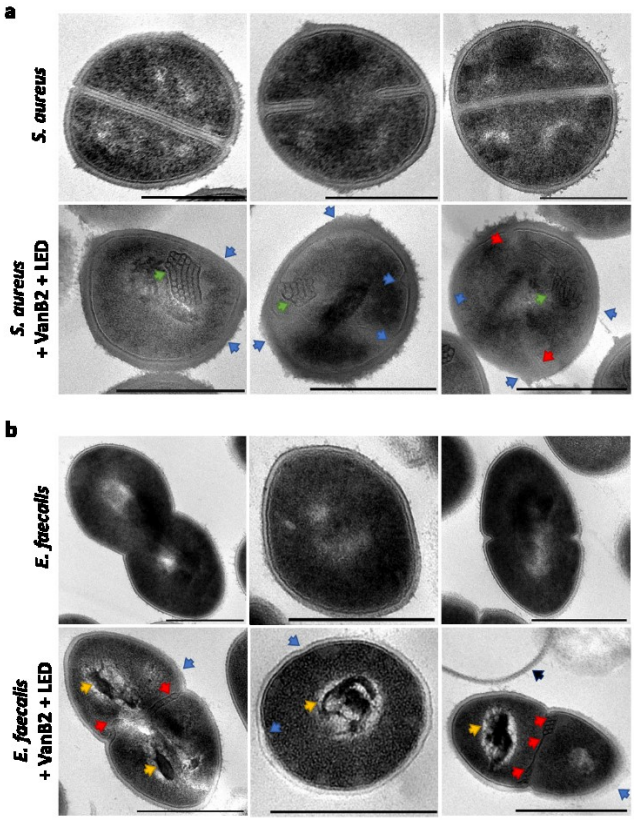

Figure 4. Transmission Electron Microscopy (TEM) of (a) *S. aureus* and (b) *E. faecalis*. Top panels: untreated controls, bottom panels: treated with VanB2 (5 μM) plus 20 min illumination (455 nm, 30 mW/cm^2). Three representative images for each condition shown. Blue arrow indicates cell envelope damage; green arrow indicates mesosome-like structure; red arrow indicates irregular septum, yellow arrow indicates electron dense areas, black arrow indicates a "ghost" cell wall. Scale bar = 500 nm.

Off-target effects of VanB2 against mammalian cells

Minimizing off-target effects of aPDT against mammalian host cells is the key challenge of PS design strategies. We assessed membrane toxicity of **VanB2** and riboflavin (0 – 50 μM) using a haemolysis assay with primary human erythrocytes (Fig. S15, a) and cell viability against HaCaT keratinocyte skin cell-line (Fig.

S15, b), both with the compound in excess. No haemolysis was observed for **VanB2** at any concentration, even with illumination. This is in contrast to 60 % erythrocyte lysis following LED activation of 50 µM riboflavin (Fig. S15, a). Riboflavin is known to accumulate within erythrocytes,[46] and the lack of haemolytic activity for **VanB2** suggests it does not accumulate within these cells.

High concentrations (50 µM) of **VanB2** after irradiation reduced the viability of the HaCaT cells by 50 %; with a comparable effect seen with 50 µM riboflavin and photo-activation. The blue-light activated riboflavin also caused ~30 % reduction in cellular viability at 5 µM, which was not observed for **VanB2** (Fig. S15, b). Since concentrations of **VanB2** of <1.25 µM were sufficient to induce complete Gram-positive bacterial killing, this shows that the lowest working concentrations of **VanB2** would have no negative impact on cellular viability.

Conclusion

The novel vancomycin-riboflavin conjugate reported here (**VanB2**) was prepared on gram scale in only two synthetic steps, and revealed both selective photo-dynamic bacterial killing, potent bactericidal activity, and an unexpected drug-release behaviour. Thanks to the triplet diradical formed upon excitation, we discovered for the first time that the flavinylethyl moiety behaves as a light-cleavable protecting groups for vancomycin, with blue light irradiation triggering an oxygen independant photochemical cascade leading to bond cleavage and drug release. In a biological context, this means that flavinyl groups can be used for light-mediated drug-release, even in cells where no oxygen is present (e.g. anaerobic bacteria, tumour tissues…), which increases versatility. In addition to their efficient photosensitizing character, flavins could therefore represent an entirely new family of “caging” compounds suitable for PDT and light-activated prodrug strategies. In the current antibacterial application, photodynamic treatment with **VanB2** was 100 % efficient against Gram-positive pathogens even when used for short-periods of time, and at sub-micromolar concentrations. Its activity was not affected by the presence of two types of resistance mechanisms, allowing eradication of ESKAPE pathogens VRE and MRSA. The conjugation strategy used here allows maximisation of the therapeutic effect of the probe by concentrating the photodynamic killing with thousands of $^1O_2$ molecules generated per PS molecule localised onto the target itself[11] thus avoiding off-target effects on mammalian cells. Thanks to the transformation of the riboflavin sub-unit into lumichrome during the light treatment, the absorption of the compound is significantly UV-shifted. This could also become a beneficial clinical attribute by preventing long-lasting sensitization of the treated area to visible light, which is a known source of painful side-effects in conventional PDT treatment[47] (i.e. internal “burning” due to the ongoing ROS generation, even in ambient light). Additionally, the conjugation of riboflavin onto the glycan moiety of vancomycin enhanced its antibacterial activity by a factor of ~10 and even helped overcome vancomycin resistance in VRE bacteria. This increases the versatility of the **VanB2** probe, which overall proved to be highly potent both in the dark and under blue light, thus making it a promising, versatile alternative in the fight against infections.[48] Future work will investigate the detailed scope and release mechanism of flavinylethyl light cleavable protecting groups.

Supporting Information

The authors have cited additional references within the Supporting Information.[49-57]

Acknowledgements

We would like to thank the Engineering and Physical Research Council (EPSRC) (grant number: EP/R018669/1 and EP/R005257/1) for funding this work. BM is recipient of UK Research and Innovation (UKRI) Future Leaders Fellowship: MR/V026097/1. We thank the Wellcome Trust Multi User Equipment Grant (WT104915MA) for supporting the TEM imaging and the CALM Imaging Facility at the University of Edinburgh. We also thank the Hill lab at the University of Nottingham for access to the *S. aureus* strain collection.

Keywords: photodynamic therapy • photolabile protecting groups • uncaging • antimicrobial resistance • antibiotic • ESKAPE pathogens

1 Majumder, M. A. A. *et al.* Antimicrobial Stewardship: Fighting Antimicrobial Resistance and Protecting Global Public Health. *Infect. Drug. Resist.* **13**, 4713-4738, doi:10.2147/idr.s290835 (2020).

2 Ventola, C. L. The Antibiotic Resistance Crisis. *Pharmacol. Ther.* **40**, 277-283 (2015).

3 Mulani, M. S., Kamble, E. E., Kumkar, S. N., Tawre, M. S. & Pardesi, K. R. Emerging Strategies to Combat ESKAPE Pathogens in the Era of Antimicrobial Resistance: A Review. *Front. Microbiol.* **10**, doi:10.3389/fmicb.2019.00539 (2019).

4 Tacconelli, E. *et al.* Discovery, research, and development of new antibiotics: the WHO priority list of antibiotic-resistant bacteria and tuberculosis. *Lancet Infect. Dis.* **18**, 318-327, doi:https://doi.org/10.1016/S1473-3099(17)30753-3 (2018).

5 Cottreau, J. M. & Christensen, A. B. Newly Approved Antimicrobials. *Orthop. Nurs.* **39** (2020).

6 Cook, M. A. & Wright, G. D. The past, present, and future of antibiotics. *Sci. Transl. Med.* **14**, eabo7793 (2022).

7 Chahine, E. B., Dougherty, J. A., Thornby, K.-A. & Guirguis, E. H. Antibiotic Approvals in the Last Decade: Are We Keeping Up With Resistance? *Ann. Pharmacother.* **56**, 441-462 (2022).

8 Nakonieczna, J. *et al.* Photoinactivation of ESKAPE pathogens: overview of novel therapeutic strategy. *Future Med. Chem.* **11**, 443-461, doi:10.4155/fmc-2018-0329 (2019).

9 Anas, A. *et al.* Advances in photodynamic antimicrobial chemotherapy. *J. Photochem. Photobiol. C: Photochem. Rev.* **49**, 100452, doi:https://doi.org/10.1016/j.jphotochemrev.2021.100452 (2021).

10 Klausen, M., Ucuncu, M. & Bradley, M. Design of Photosensitizing Agents for Targeted Antimicrobial Photodynamic Therapy. *Molecules* **25**, 5239, doi:10.3390/molecules25225239 (2020).

11 DeRosa, M. Photosensitized singlet oxygen and its applications. *Coord. Chem. Rev.* **233-234**, 351-371, doi:10.1016/S0010-8545(02)00034-6 (2002).

12 Plaetzer, K., Krammer, B., Berlanda, J., Berr, F. & Kiesslich, T. Photophysics and photochemistry of photodynamic therapy: fundamental aspects. *Lasers Med. Sci.* **24**, 259-268, doi:10.1007/s10103-008-0539-1 (2009).

13 Nonell, S., Flors, C. & Royal Society of, C. *Singlet oxygen: applications in biosciences and nanosciences*. Vol. 13-14 (Royal Society of Chemistry, 2016).

14 dos Santos, A. F., de Almeida, D. R. Q., Terra, L. F., Baptista, M. S. & Labriola, L. Photodynamic therapy in cancer treatment - an update review. *J. Cancer Metastatis Treat.* **5**, 25, doi:10.20517/2394-4722.2018.83 (2019).

15 Tampa, M. *et al.* Photodynamic therapy: A hot topic in dermato-oncology. *Oncol. Lett.* **17**, 4085-4093, doi:10.3892/ol.2019.9939 (2019).

16 Tandon, Y. K., Yang, M. F. & Baron, E. D. Role of photodynamic therapy in psoriasis: a brief review. *Photodermatology, photoimmunology & photomedicine* **24**, 222-230 (2008).

17 Plotino, G., Grande, N. M. & Mercade, M. Photodynamic therapy in endodontics. *Int Endod J* **52**, 760-774, doi:10.1111/iej.13057 (2019).

18 Zhao, T., Song, J., Ping, Y. & Li, M. The Application of Antimicrobial Photodynamic Therapy (aPDT) in the Treatment of Peri-Implantitis. *Comput. Math. Methods Med.* **2022**, 3547398, doi:10.1155/2022/3547398 (2022).

19 Tavares, A. *et al.* Antimicrobial Photodynamic Therapy: Study of Bacterial Recovery Viability and Potential Development of Resistance after Treatment. *Mar. Drugs* **8**, 91-105, doi:10.3390/md8010091 (2010).

20 Tim, M. Strategies to optimize photosensitizers for photodynamic inactivation of bacteria. *J. Photochem. Photobiol. B: Biol.* **150**, 2-10 (2015).

21 Wainwright, M., Phoenix, D. A., Marland, J., Wareing, D. R. A. & Bolton, F. J. A study of photobactericidal activity in the phenothiazinium series. *FEMS Microbiol. Immunol.* **19**, 75-80, doi:10.1111/j.1574-695X.1997.tb01074.x (1997).

22 Merchat, M., Spikes, J. D., Bertoloni, G. & Jori, G. Studies on the mechanism of bacteria photosensitization by meso-substituted cationic porphyrins. *J. Photochem. Photobiol. B: Biol.* **35**, 149-157, doi:10.1016/S1011-1344(96)07321-6 (1996).

23 Li, M. *et al.* Photodynamic antimicrobial chemotherapy with cationic phthalocyanines against Escherichia coli planktonic and biofilm cultures. *RSC Adv.* **7**, 40734-40744, doi:10.1039/C7RA06073D (2017).

24 Oniszczuk, A., Wojtunik-Kulesza, K. A., Oniszczuk, T. & Kasprzak, K. The potential of photodynamic therapy (PDT)—Experimental investigations and clinical use. *Biomedicine & Pharmacotherapy* **83**, 912-929 (2016).

25 Cieplik, F. *et al.* Antimicrobial photodynamic therapy–what we know and what we don't. *Critical Reviews in Microbiology* **44**, 571-589 (2018).

26 Ucuncu, M. *et al.* Polymyxin-based photosensitizer for the potent and selective killing of Gram-negative bacteria. *Chem. Commun.* **56**, 3757-3760, doi:10.1039/d0cc00155d (2020).

27 Krishna, C. M., Uppuluri, S., Riesz, P., Jr, J. S. Z. & Balasubramanian, D. A study of the photodynamic efficiencies of some eye lens constituents. *Photochem Photobiol* **54**, 51-58, doi:10.1111/j.1751-1097.1991.tb01984.x (1991).

28 Weinstain, R., Slanina, T., Kand, D. & Klán, P. Visible-to-NIR-Light Activated Release: From Small Molecules to Nanomaterials. *Chem. Rev.*, doi:10.1021/acs.chemrev.0c00663 (2020).

29 Klausen, M. & Blanchard-Desce, M. Two-photon uncaging of bioactive compounds: Starter guide to an efficient IR light switch. *J. Photochem. Photobiol. C: Photochem. Rev.* **48**, 100423, doi:10.1016/j.jphotochemrev.2021.100423 (2021).

30 Smith, E. C. & Metzler, D. E. The Photochemical Degradation of Riboflavin. *J. Am. Chem. Soc.* **85**, 3285-3288, doi:10.1021/ja00903a051 (1963).

31 Song, P.-S., Smith, E. C. & Metzler, D. E. Photochemical Degradation of Flavins. II. The Mechanism of Alkaline Hydrolysis of 6,7-Dimethyl-9-formylmethylisoalloxazine1,2. *J. Am. Chem. Soc.* **87**, 4181-4184, doi:10.1021/ja01096a031 (1965).

32 Blaskovich, M. A. T. *et al.* Developments in Glycopeptide Antibiotics. *ACS Infect. Dis.* **4**, 715-735, doi:10.1021/acsinfecdis.7b00258 (2018).

33 Mills, B. *et al.* Molecular detection of Gram-positive bacteria in the human lung through an optical fiber–based endoscope. *Eur. J. Nucl. Med. Mol. Imaging*, doi:10.1007/s00259-020-05021-4 (2020).

34 Drössler, P., Holzer, W., Penzkofer, A. & Hegemann, P. pH dependence of the absorption and emission behaviour of riboflavin in aqueous solution. *Chem. Phys.* **282**, 429-439, doi:10.1016/S0301-0104(02)00731-0 (2002).

35 Lutkus, L. V., Rickenbach, S. S. & McCormick, T. M. Singlet oxygen quantum yields determined by oxygen consumption. *J. Photochem. Photobiol. A* **378**, 131-135, doi:https://doi.org/10.1016/j.jphotochem.2019.04.029 (2019).

36 Hatchard, C. G., Parker, C. A. & Bowen, E. J. A new sensitive chemical actinometer - II. Potassium ferrioxalate as a standard chemical actinometer. *Proc. R. Soc. Lond. A* **235**, 518-536, doi:10.1098/rspa.1956.0102 (1956).

37 Holzer, W. *et al.* Photo-induced degradation of some flavins in aqueous solution. *Chem. Phys.* **308**, 69-78, doi:https://doi.org/10.1016/j.chemphys.2004.08.006 (2005).

38 Tian, Y., Chong, X., Yao, S. & Xu, M. Spectral Data Analysis and Identification of Vancomycin Hydrochloride. *Front. Chem.* **9**, doi:10.3389/fchem.2021.753060 (2021).

39 Cetinkaya, Y., Falk, P. & Mayhall, C. G. Vancomycin-Resistant Enterococci. *Clin. Microbiol. Rev.* **13**, 686-707, doi:10.1128/CMR.13.4.686 (2000).

40 Gupta, V., Singla, N., Behl, P., Sahoo, T. & Chander, J. Antimicrobial susceptibility pattern of vancomycin resistant enterococci to newer antimicrobial agents. *Indian J. Med. Res.* **141** (2015).

41 Staerck, C. *et al.* The Glycosylphosphatidylinositol-Anchored Superoxide Dismutase of Scedosporium apiospermum Protects the Conidia from Oxidative Stress. *J. Fungi* **7** (2021).

42 Askoura, M., Yousef, N., Mansour, B. & Yehia, F. A.-z. A. Antibiofilm and staphyloxanthin inhibitory potential of terbinafine against Staphylococcus aureus: in vitro and in vivo studies. *Ann. Clin. Microbiol. Antimicrob.* **21**, 21, doi:10.1186/s12941-022-00513-7 (2022).

43 Clauditz, A., Resch, A., Wieland, K.-P., Peschel, A. & Götz, F. Staphyloxanthin Plays a Role in the Fitness of Staphylococcus aureus and Its Ability To Cope with Oxidative Stress. *Infect. Immun.* **74**, 4950-4953, doi:10.1128/IAI.00204-06 (2006).

44 Esmail, M. A. M., Abdulghany, H. M. & Khairy, R. M. M. Prevalence of Multidrug-Resistant Enterococcus faecalis in Hospital-Acquired Surgical Wound Infections and Bacteremia: Concomitant Analysis of Antimicrobial Resistance Genes. *Infect. Dis: Res. Treat.* **12**, 1178633719882929, doi:10.1177/1178633719882929 (2019).

45 Grigor'eva, A. *et al.* Changes in the Ultrastructure of Staphylococcus aureus Treated with Cationic Peptides and Chlorhexidine. *Microorganisms* **8** (2020).

46 Efsa Panel on Dietetic Products, N. *et al.* Dietary Reference Values for riboflavin. *EFSA J.* **15**, e04919, doi:https://doi.org/10.2903/j.efsa.2017.4919 (2017).

47 Fink, C., Enk, A. & Gholam, P. Photodynamic therapy – Aspects of pain management. *J. Dtsch. Dermatol. Ges.* **13**, 15-22, doi:https://doi.org/10.1111/ddg.12546 (2015).

48 Willis, J. A. *et al.* Breaking down antibiotic resistance in methicillin-resistant Staphylococcus aureus: Combining antimicrobial photodynamic and antibiotic treatments. *Proc. Natl. Acad. Sci. U. S. A.* **119**, e2208378119, doi:10.1073/pnas.2208378119 (2022).

49 Würth, C., Grabolle, M., Pauli, J., Spieles, M. & Resch-Genger, U. Relative and absolute determination of fluorescence quantum yields of transparent samples. *Nat. Protoc.* **8**, 1535-1550, doi:10.1038/nprot.2013.087 (2013).

50 Resch-Genger, U. & Rurack, K. Determination of the photoluminescence quantum yield of dilute dye solutions (IUPAC Technical Report). *Pure Appl. Chem.* **85**, 2005-2013, doi:10.1351/PAC-REP-12-03-03 (2013).

51 Brouwer, A. M. Standards for photoluminescence quantum yield measurements in solution (IUPAC Technical Report). *Pure Appl. Chem.* **83**, 2213-2228, doi:10.1351/PAC-REP-10-09-31 (2011).

52 Adarsh, N., Avirah, R. R. & Ramaiah, D. Tuning Photosensitized Singlet Oxygen Generation Efficiency of Novel Aza-BODIPY Dyes. *Org. Lett.* **12**, 5720-5723, doi:10.1021/ol102562k (2010).

53 Baier, J. *et al.* Singlet Oxygen Generation by UVA Light Exposure of Endogenous Photosensitizers. *Biophys. J.* **91**, 1452-1459, doi:10.1529/biophysj.106.082388 (2006).

54 Chacon, J. N., McLearie, J. & Sinclair, R. S. Singlet oxygen yields and radical contributions in the dye-sensitised photo-oxidation in methanol of esters of polyunsaturated fatty acids (oleic, linoleic, linolenic and arachidonic). *Photochem Photobiol* **47**, 647-656, doi:10.1111/j.1751-1097.1988.tb02760.x (1988).

55 Furuta, T. *et al.* Brominated 7-hydroxycoumarin-4-ylmethyls: Photolabile protecting groups with biologically useful cross-sections for two photon photolysis. *Proc. Natl. Acad. Sci. U.S.A.* **96**, 1193-1200, doi:10.1073/pnas.96.4.1193 (1999).

56 Montalti, M., Credi, A., Prodi, L. & Gandolfi, M. T. in *Handbook of Photochemistry* Ch. 12, 601-611 (CRC Press, 2006).

57 Murahashi, S.-I. *et al.* Flavin-catalyzed aerobic oxidation of sulfides and thiols with formic acid/triethylamine. *Chem. Commun.* **50**, 10295-10298, doi:10.1039/C4CC05216A (2014).